ISSN 1070-3284, Russian Journal of Coordination Chemistry, 2009, Vol. 35, No. 3, pp. 170–178. © Pleiades Publishing, Ltd., 2009.
Original Russian Text © T.A. Rodina, A.V. Ivanov, O.A. Bredyuk, A.V. Gerasimenko, 2009, published in Koordinatsionnaya Khimiya, 2009, Vol. 35, No. 3, pp. 172–180.

Synthesis, Structure, and Thermal Properties of Tallium(I) N,N-*cyclo*-Pentamethylenedithiocarbamate $[Tl_2\{S_2CN(CH_2)_5\}_2]_n$: X-Ray Diffraction, ^{13}C and ^{15}N MAS NMR, and Thermal Analysis Studies (An Example of Complicated Structural Organization)

T. A. Rodina[a], A. V. Ivanov[b], O. A. Bredyuk[b], and A. V. Gerasimenko[c]

[a]*Amur State University, 21 ul. Ignat'eva, Blagoveshchensk, 675027 Russia*

[b]*Institute of Geology and Nature Management, Far East Division, Russian Academy of Sciences, Blagoveshchensk, 675000 Russia*

[c] *Institute of Chemistry, Far East Division, Russian Academy of Sciences, pr. Stoletiya Vladivostoka 159, Vladivostok, 690022 Russia*

e-mail: alexander.v.ivanov@chemist.com

Received May 28, 2008

Abstract—Crystalline polynuclear thallium(I) N,N-*cyclo*-pentamethylenedithiocarbamate is synthesized by the preparative synthesis. According to the MAS NMR (^{13}C, ^{15}N) data, its composition includes four structurally nonequivalent dithiocarbamate ligands. According to the X-ray diffraction data, the complex synthesized is a remarkable example for the self-organization of the chemical system with a simple composition into an unusually complicated structure. The latter includes three types of the nonequivalent binuclear molecules $[Tl_2\{S_2CN(CH_2)_5\}_2]$ (**I**) performing various structural functions. Two of them (centrosymmetric) alternate and participate in infinite polymeric chain building. The third structural function (noncentrosymmetric) is associated with the joining of the polymeric chains into two-dimensional layers. Structurally nonequivalent binuclear molecules **I** are shown to be related as conformers. The study of the thermal properties of the complex shows that Tl_2S is the final thermal destruction product.

DOI: 10.1134/S1070328409030026

INTRODUCTION

We reported previously [1] the synthesis and structure of the first representative of the thallium(I) complexes with the cyclic N,N-hexamethylenedithiocarbamate ligand. The structural type of the complex was found to correspond, as a whole, to other earlier described thallium(I) dialkyldithiocarbamates [2–7]. The binuclear molecules $[Tl_2\{S_2CN(CH_2)_6\}_2]$ joined into polymeric chains are the main structural units. In turn, the chains form layers. According to the X-ray diffraction [1–7] and ^{13}C and ^{15}N MAS NMR [1] data, most of the Tl(I) compounds discussed are characterized by structural equivalency of the dialkyldithiocarbamate ligands.

In this work, we synthesized a new crystalline polymeric tallium(I) N,N-*cyclo*-pentamethylenedithiocarbamate (PmDtc) complex $[Tl_2\{S_2CN(CH_2)_5\}_2]_n$ (**I**), whose structure and thermal properties were studied by the data of X-ray diffraction analysis, solid-state high-resolution ^{13}C and ^{15}N CP/MAS NMR spectroscopy, and combined thermal analysis. Complex **I** is a remarkable example for the self-organization of the chemical system of relatively simple composition into the unusually complicated structure including three types of nonequivalent binuclear molecules that perform various functions. It was found that Tl_2S was the final product of the thermal destruction of the complex.

EXPERIMENTAL

Synthesis. Compound **I** was synthesized by the interaction of equimolar aqueous solutions of $TlNO_3$ (acidified with nitric acid to pH 3.5) and $Na\{S_2CN(CH_2)_5\} \cdot 2H_2O$. The bulky light yellow precipitate was filtered off, washed, and dried on the filter. The yield was 87%. The yellow lustrous single crystals of compound **I** (mp = 176–178°C) were isolated from hot (~60°C) toluene.

The ^{13}C and ^{15}N MAS NMR spectra of complex I were recorded on a CMX-360 pulse spectrometer (Varian/Chemagnetics InfinityPlus, United States) with working frequencies of 90.52 and 36.48 MHz, a superconducting magnet (B_0 = 8.46 T), and Fourier transformation. When recording the spectra, the proton cross-polarization effect was used. Proton decoupling using the radio-frequency field at the resonance frequency of protons was applied for ^{13}C–^{1}H and ^{15}N–^{1}H dipole–dipole interaction decoupling [8]. For ^{13}C and ^{15}N NMR

measurements, complex **I** (~350 mg) was placed in a ZrO_2 ceramic rotor 7.5 mm in diameter. Magic-angle-spinning was carried out at frequencies of 5400 and 4200(1) Hz, the accumulation number was 5200/7800, the duration of proton π/2 pulses was 6.0/6.0 μs, the ^1H–^{13}C/^1H–^{15}N contact time was 2.0/3.0 ms, and the interval between excitation pulses was 10.0/10.0 s. Isotropic ^{13}C chemical shifts are given in ppm relative to one of the components of the external standard, which was crystalline adamantane [9] (δ = 38.48 ppm relative to tetramethylsilane [10]), and those of ^{15}N are given relative to crystalline NH_4Cl (0 ppm, –341 ppm in the absolute scale [11]). The magnetic field homogeneity was monitored using the reference line width of adamantane: 2.6 Hz. During the experiments, the chemical shifts were corrected to the mafnetic field drift, whose frequency equivalent for the ^{13}C/^{15}N nuclei was 0.098/0.033 Hz/h. To refine the chemical shifts and integral intensities of overlapped resonance signals, the fragment-to-fragment mathematical simulation of the spectra was used. The simulation took into account the position and width of the lines and the contribution of the Lorentzian and Gaussian components to the line shape.

The X-ray diffraction analysis of crystal **I** was carried out on a BRUKER SMART 1000 CCD diffractometer (MoK_α radiation, λ = 0.71073 Å, graphite monochromator) at 173(1) K. The data were collected in the hemisphere area [12] (the crystal–detector distance was 50 mm) in the ω scan mode with an increment of 0.2° and an exposure of 30 s per frame. The X-ray absorption correction of the sample was applied by equivalent reflection indices. Structure **I** was determined by a direct method and refined by the least-squares method (for F^2) in the full-matrix anisotropic approximation of non-hydrogen atoms. The positions of hydrogen atoms were calculated geometrically and included into refinement by the riding model. The data were collected and edited and the unit cell parameters were refined using the SMART and SAINT-*Plus* programs [12]. All calculations on the determination and refinement of structure **I** were performed using the SHELXTL/PC program packages [13]. The coordinates of atoms, bond lengths, and angles were deposited with the Cambridge Crystallographic Data Centre (no. 687 111).

The main crystallographic data and refinement results for structure **I** are presented in Table 1. Selected bond lengths and angles are given in Table 2.

The thermal properties of complex **I** were studied by the method of combined thermal analysis including the simultaneous detection of thermogravimetry (TG) and differential scanning calorimetry (DSC) curves. The study was carried out with an STA 449C Jupiter instrument (NETZSCH) in quartz crucibles closed with caps containing a hole providing a vapor pressure of 1 atm during the thermal decomposition of the sample. The heating rate was 5 K/min to 480°C under an argon atmosphere. The choice of the limiting heating temperature is caused by the fact that Tl_2S melts at 449 or 452°C (depending on the method of preparation) [14]. The weighed sample was 20.33 mg. The accuracy of temperature measurements was ±1°C, and that of the weight change was $\pm 1 \times 10^{-2}$ mg.

Table 1. Crystallographic data, experimental parameters, and refinement details for the $[Tl_2\{S_2CN(CH_2)_5\}_2]_n$ structure (**I**)

Parameter	Value
Empirical formula	$C_{12}H_{20}N_2S_4Tl_2$
FW	729.28
Crystal system	Monoclinic
Space group	$P2_1/c$
a, Å	9.951(1)
b, Å	11.897(2)
c, Å	30.758(4)
β, deg	90.166(3)
V, Å^3	3641.4(8)
Z	8
ρ_{calcd}, g/cm^3	2.661
μ, mm^{-1}	18.129
F(000)	2656
Crystal shape (size, mm)	Prism (0.27 × 0.05 × 0.02)
θ range, deg	2.05–25.02
Interval of reflection indices	$-10 \le h \le 11$, $-14 \le k \le 13$, $-23 \le l \le 36$
Measured reflections	16709
Independent reflections	6410 (R_{int} = 0.0577)
Reflections with $I > 2\sigma(I)$	4763
Refinement variables	362
Goodness-of-fit	1.011
R factors for $F^2 > 2\sigma(F^2)$	R_1 = 0.0440, wR_2 = 0.0857
R factors for all reflections	R_1 = 0.0700, wR_2 = 0.0940
Extinction coefficient	0.00006(2)
Residual electron density (min/max), e Å^{-3}	–1.438/1.786

Table 2. Bond lengths (d), bond angles (ω), and torsion angles (φ) in the $[Tl_2\{S_2CN(CH_2)_5\}_2]_n$ structure*

Molecule A

Bond	d, Å	Bond	d, Å	Bond	d, Å
Tl(1)–S(1)	2.962(3)	Tl(2)–S(2)[c]	4.125(3)	N(2)–C(12)	1.468(13)
Tl(1)–S(2)	3.152(3)	S(1)–C(1)	1.737(11)	C(2)–C(3)	1.52(2)
Tl(1)–S(3)	3.032(3)	S(2)–C(1)	1.718(11)	C(3)–C(4)	1.49(2)
Tl(1)–S(4)	3.278(3)	S(3)–C(7)	1.739(10)	C(4)–C(5)	1.53(2)
Tl(1)–S(5)	3.447(3)	S(4)–C(7)	1.715(12)	C(5)–C(6)	1.52(2)
Tl(1)–S(7)[a]	3.427(3)	N(1)–C(1)	1.331(13)	C(8)–C(9)	1.51(2)
Tl(2)–S(1)	3.128(3)	N(1)–C(2)	1.447(13)	C(9)–C(10)	1.52(2)
Tl(2)–S(2)	3.047(3)	N(1)–C(6)	1.499(13)	C(10)–C(11)	1.50(2)
Tl(2)–S(3)	3.026(3)	N(2)–C(7)	1.327(13)	C(11)–C(12)	1.52(2)
Tl(2)–S(4)	2.979(3)	N(2)–C(8)	1.46(1)		
Angle	ω, deg	Angle	ω, deg	Angle	ω, deg
S(1)Tl(1)S(2)	57.88(8)	S(2)Tl(2)S(2)[c]	134.59(4)	Tl(1)S(3)Tl(3)	95.27(7)
S(1)Tl(1)S(3)	83.99(8)	S(3)Tl(2)S(2)[c]	115.89(7)	Tl(2)S(3)Tl(3)	101.16(7)
S(1)Tl(1)S(4)	106.82(9)	S(4)Tl(2)S(2)[c]	116.05(7)	C(7)S(4)Tl(1)	80.8(4)
S(2)Tl(1)S(4)	77.06(7)	C(1)S(1)Tl(1)	90.2(4)	C(7)S(4)Tl(2)	87.7(4)
S(3)Tl(1)S(2)	106.44(8)	C(1)S(1)Tl(2)	82.0(4)	Tl(2)S(4)Tl(1)	70.18(6)
S(3)Tl(1)S(4)	55.77(8)	S(2)C(1)S(1)	118.1(6)	C(1)N(1)C(2)	124.2(9)
S(1)Tl(1)S(7)[a]	97.03(8)	N(1)C(2)C(3)	111.8(9)	C(1)N(1)C(6)	123.2(9)
S(3)Tl(1)S(7)[a]	148.32(8)	C(4)C(3)C(2)	110.0(11)	C(2)N(1)C(6)	112.5(8)
S(2)Tl(1)S(7)[a]	100.63(7)	C(3)C(4)C(5)	110.9(10)	C(7)N(2)C(8)	124.1(9)
S(4)Tl(1)S(7)[a]	149.27(7)	C(6)C(5)C(4)	111.2(10)	C(7)N(2)C(12)	123.9(9)
S(1)Tl(1)S(5)	67.35(8)	N(1)C(6)C(5)	108.7(9)	C(8)N(2)C(12)	112.0(8)
S(2)Tl(1)S(5)	124.06(7)	Tl(1)S(1)Tl(2)	72.55(7)	N(1)C(1)S(2)	121.0(8)
S(3)Tl(1)S(5)	76.83(8)	C(1)S(1)Tl(4)[b]	97.6(4)	N(1)C(1)S(1)	120.9(8)
S(4)Tl(1)S(5)	132.50(7)	Tl(1)S(1)Tl(4)[b]	79.74(8)	N(2)C(7)S(4)	121.6(8)
S(5)Tl(1)S(7)[a]	74.49(7)	Tl(2)S(1)Tl(4)[b]	152.28(10)	N(2)C(7)S(3)	120.5(9)
S(2)Tl(2)S(1)	57.34(8)	C(1)S(2)Tl(2)	84.8(4)	S(4)C(7)S(3)	117.9(6)
S(3)Tl(2)S(1)	81.32(8)	C(1)S(2)Tl(1)	84.4(4)	N(2)C(8)C(9)	112.4(10)
S(3)Tl(2)S(2)	109.30(8)	Tl(2)S(2)Tl(1)	71.09(6)	C(8)C(9)C(10)	109.7(10)
S(4)Tl(2)S(1)	110.36(8)	C(7)S(3)Tl(2)	85.84)	C(11)C(10)C(9)	110.6(9)
S(4)Tl(2)S(2)	83.35(8)	C(7)S(3)Tl(1)	88.3(4)	C(10)C(11)C(12)	111.5(9)
S(4)Tl(2)S(3)	59.04(8)	Tl(2)S(3)Tl(1)	73.05(7)	N(2)C(12)C(11)	110.4(9)
S(1)Tl(2)S(2)[c]	132.89(7)	C(7)S(3)Tl(3)	172.9(4)		
Angle	φ, deg	Angle	φ, deg	Angle	φ, deg
S(1)C(1)N(1)C(2)	–179.4(9)	S(3)C(7)N(2)C(8)	–2(2)	C(1)S(1)S(2)Tl(1)	144.9(7)
S(2)C(1)N(1)C(6)	–175.8(9)	S(3)Tl(2)C(7)S(4)	–149.7(6)	S(4)C(7)N(2)C(12)	–5(2)
S(1)Tl(1)C(1)S(2)	–150.0(6)	S(1)C(1)N(1)C(6)	5(2)	S(4)C(7)N(2)C(8)	175.6(9)
S(3)C(7)N(2)C(12)	178.2(9)	S(2)C(1)N(1)C(2)	0(2)	C(7)S(3)S(4)Tl(2)	144.4(8)

Molecule B

Bond	d, Å	Bond	d, Å	Bond	d, Å
Tl(3)–S(5)	3.024(3)	Tl(3)–S(8)	3.653(3)	N(3)–C(14)	1.48(1)
Tl(3)–S(5)[b]	3.052(3)	S(5)–C(13)	1.749(11)	C(14)–C(15)	1.51(2)
Tl(3)–S(6)	2.980(3)	S(6)–C(13)	1.730(11)	C(15)–C(16)	1.49(2)
Tl(3)–S(6)[b]	3.173(3)	N(3)–C(13)	1.305(13)	C(16)–C(17)	1.52(2)
Tl(3)–S(3)	4.180(3)	N(3)–C(18)	1.45(1)	C(17)–C(18)	1.49(2)

Table 2. (Contd.)

Molecule B

Angle	ω, deg	Angle	ω, deg	Angle	ω, deg
S(5)Tl(3)S(5)^{b}	104.33(7)	S(6)^{b}Tl(3)S(3)	100.60(7)	Tl(3)S(6)Tl(3)^{b}	74.48(7)
S(5)Tl(3)S(6)^{b}	56.97(8)	S(8)Tl(3)S(3)	116.07(6)	C(13)N(3)C(18)	126.0(9)
S(5)^{b}Tl(3)S(6)^{b}	76.21(8)	C(13)S(5)Tl(3)	87.3(4)	C(13)N(3)C(14)	123.1(10)
S(6)Tl(3)S(5)	79.57(8)	C(13)S(5)Tl(3)^{b}	84.3(4)	C(18)N(3)C(14)	110.6(9)
S(6)Tl(3)S(5)^{b}	58.73(8)	Tl(3)S(5)Tl(3)^{b}	75.67(7)	N(3)C(13)S(6)^{b}	121.4(8)
S(6)Tl(3)S(6)^{b}	105.52(7)	C(13)S(5)Tl(4)^{b}	129.0(4)	N(3)C(13)S(5)	122.1(8)
S(5)Tl(3)S(8)	170.74(7)	Tl(3)S(5)Tl(4)^{b}	128.07(9)	S(6)^{b}C(13)S(5)	116.5(6)
S(5)^{b}Tl(3)S(8)	72.80(7)	Tl(3)^{b}S(5)Tl(4)^{b}	73.38(6)	N(3)C(14)C(15)	110.6(10)
S(6)Tl(3)S(8)	91.56(7)	Tl(3)S(5)Tl(1)	112.46(9)	C(16)C(15)C(14)	109.8(11)
S(6)^{b}Tl(3)S(8)	129.09(7)	Tl(3)^{b}S(5)Tl(1)	153.07(10)	C(15)C(16)C(17)	110.0(10)
S(5)Tl(3)S(3)	65.94(7)	Tl(4)^{b}S(5)Tl(1)	82.28(6)	C(18)C(17)C(16)	111.1(10)
S(5)^{b}Tl(3)S(3)	169.31(7)	C(13)^{b}S(6)Tl(3)	86.9(4)	N(3)C(18)C(17)	110.5(10)
S(6)Tl(3)S(3)	113.38(7)	C(13)^{b}S(6)Tl(3)^{b}	82.9(4)		
Angle	φ, deg	Angle	φ, deg	Angle	φ, deg
S(5)C(13)N(3)C(18)	177.7(9)	S(5)Tl(3)^{b}C(13)S(6)^{b}	–144.2(6)	S(6)^{b}C(13)N(3)C(14)	–176.3(9)
S(6)^{b}C(13)N(3)C(18)	–3(2)	S(5)C(13)N(3)C(14)	4(2)	C(13)S(5)S(6)^{b}Tl(3)^{b}	138.0(7)

Molecule C

Bond	*d*, Å	Bond	*d*, Å	Bond	*d*, Å
Tl(4)–S(7)	3.150(3)	Tl(4)–S(5)^{b}	3.350(3)	N(4)–C(24)	1.48(1)
Tl(4)–S(7)^{d}	2.915(3)	S(7)–C(19)	1.727(12)	C(20)–C(21)	1.51(2)
Tl(4)–S(8)	3.086(3)	S(8)–C(19)	1.696(11)	C(21)–C(22)	1.54(2)
Tl(4)–S(8)^{d}	3.259(3)	N(4)–C(19)	1.36(1)	C(22)–C(23)	1.50(1)
Tl(4)–S(1)^{b}	3.920(3)	N(4)–C(20)	1.481(13)	C(23)–C(24)	1.51(2)
Angle	ω, deg	Angle	ω, deg	Angle	ω, deg
S(7)Tl(4)S(8)	56.67(7)	S(8)^{d}Tl(4)S(1)^{b}	103.28(7)	Tl(4)^{d}S(8)Tl(3)	140.11(10)
S(7)Tl(4)S(8)^{d}	76.79(8)	S(5)^{b}Tl(4)S(1)^{b}	58.32(7)	C(19)N(4)C(20)	123.9(9)
S(7)^{d}Tl(4)S(7)	104.08(7)	C(19)S(7)Tl(4)^{d}	90.2(4)	C(19)N(4)C(24)	122.9(9)
S(7)^{d}Tl(4)S(8)	83.07(8)	C(19)S(7)Tl(4)	83.6(4)	C(20)N(4)C(24)	112.5(9)
S(7)^{d}Tl(4)S(8)^{d}	56.97(7)	Tl(4)^{d}S(7)Tl(4)	75.92(7)	N(4)C(19)S(8)	121.6(8)
S(8)Tl(4)S(8)^{d}	107.94(7)	C(19)S(7)Tl(1)^{e}	104.1(4)	N(4)C(19)S(7)	118.6(8)
S(7)Tl(4)S(5)^{b}	131.08(7)	Tl(4)^{d}S(7)Tl(1)^{e}	89.31(8)	S(8)C(19)S(7)	119.8(7)
S(7)^{d}Tl(4)S(5)^{b}	82.91(8)	Tl(4)S(7)Tl(1)^{e}	163.48(10)	N(4)C(20)C(21)	110.7(9)
S(8)Tl(4)S(5)^{b}	76.91(7)	C(19)S(8)Tl(4)	86.1(4)	C(20)C(21)C(22)	112.1(9)
S(8)^{d}Tl(4)S(5)^{b}	137.64(7)	C(19)S(8)Tl(4)^{d}	79.6(4)	C(23)C(22)C(21)	109.1(9)
S(7)Tl(4)S(1)^{b}	165.13(7)	Tl(4)S(8)Tl(4)^{d}	72.06(7)	C(22)C(23)C(24)	112.3(9)
S(7)^{d}Tl(4)S(1)^{b}	87.84(7)	C(19)S(8)Tl(3)	90.7(4)	N(4)C(24)C(23)	110.3(9)
S(8)Tl(4)S(1)^{b}	135.10(7)	Tl(4)S(8)Tl(3)	68.71(6)		*
Angle	φ, deg	Angle	φ, deg	Angle	φ, deg
S(7)C(19)N(4)C(24)	173.6(8)	S(7)Tl(4)C(19)S(8)	144.6(6)	S(8)C(19)N(4)C(24)	–8(2)
S(8)C(19)N(4)C(20)	–177.5(8)	S(7)C(19)N(4)C(20)	4(2)	C(19)S(7)S(8)Tl(4)	–136.7(7)

* The symmetry operation codes: [a] *x*, *y* + 1, *z*; [b] –*x*, –*y*, –*z* + 2; [c] –*x*, *y* – 1/2, –*z* + 3/2; [d] –*x*, –*y* – 1, –*z* + 2; [e] *x*, *y* – 1, *z*.

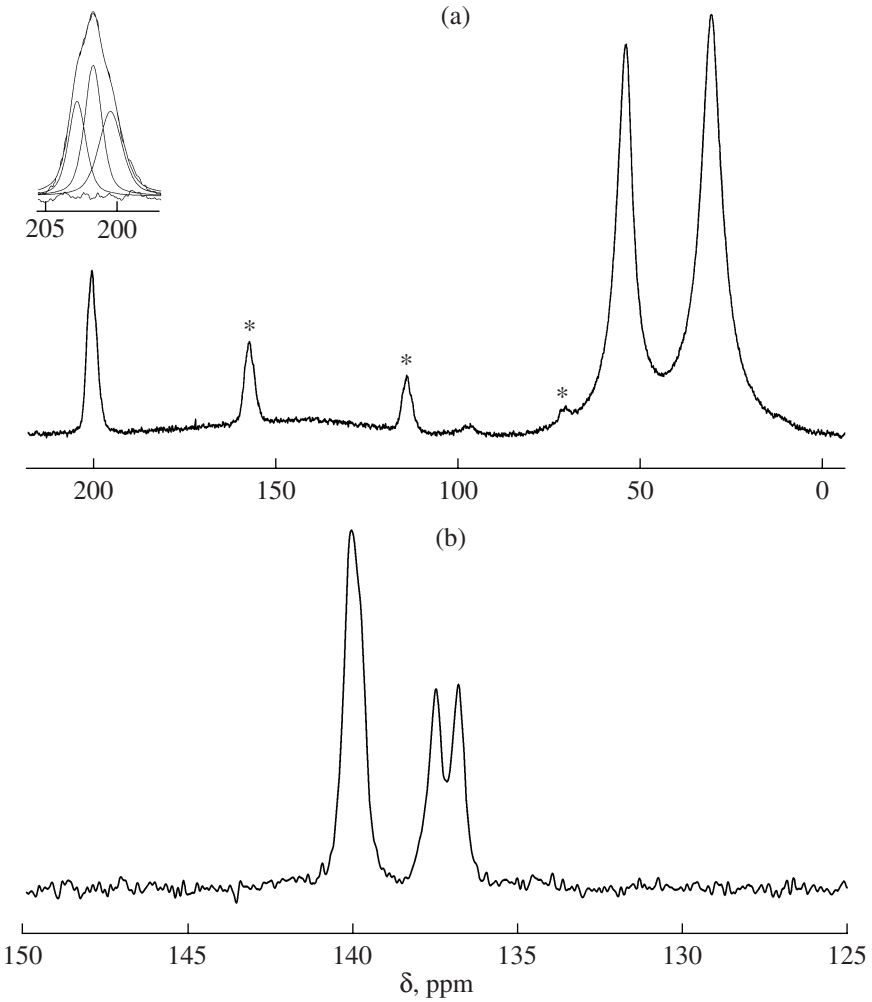

Fig. 1. (a) ^{13}C and (b) ^{15}N NMR spectra of polycrystalline complex **I** (sidebands are marked with arrows). The number of accumulations/rotation frequency of samples (Hz) was (a) 5200/5400 and (b) 7800/4200.

RESULTS AND DISCUSSION

The ^{13}C MAS NMR spectrum of crystalline complex **I** (Fig. 1a, Table 3) includes the resonance signals of the =NC(S)S–, $=NCH_2–$, and $–CH_2–$ groups of the PmDtc ligands. Since the region of the =NC(S)S groups is most informative in the structural respect for the dialkyldithiocarbamate complexes [15–17], the mathematical simulation was carried out for the ^{13}C resonance signal with

Table 3. Chemical shifts (δ, ppm) of the ^{13}C and ^{15}N NMR signals for compounds **I** and **Ia** relative to tetramethylsilane and NH_4Cl

Compound	δ ^{13}C			δ ^{15}N
	$–S_2CN=$	$=NCH_2–$	$–CH_2–$	–N=
$[Tl_2\{S_2CN(CH_2)_5\}_2]_n$ (**I**)	202.7 201.5 200.3 (1 : 2 : 1)	51.8	27.9	140.1 139.9 137.6 136.9 (1 : 1) : (1 : 1)
$Na\{S_2CN(CH_2)_5\} \cdot 2H_2O$ (**Ia**)	205.2	54.6, 53.3 (1 : 1)	27.4, 27.1 (2 : 1)	135.1

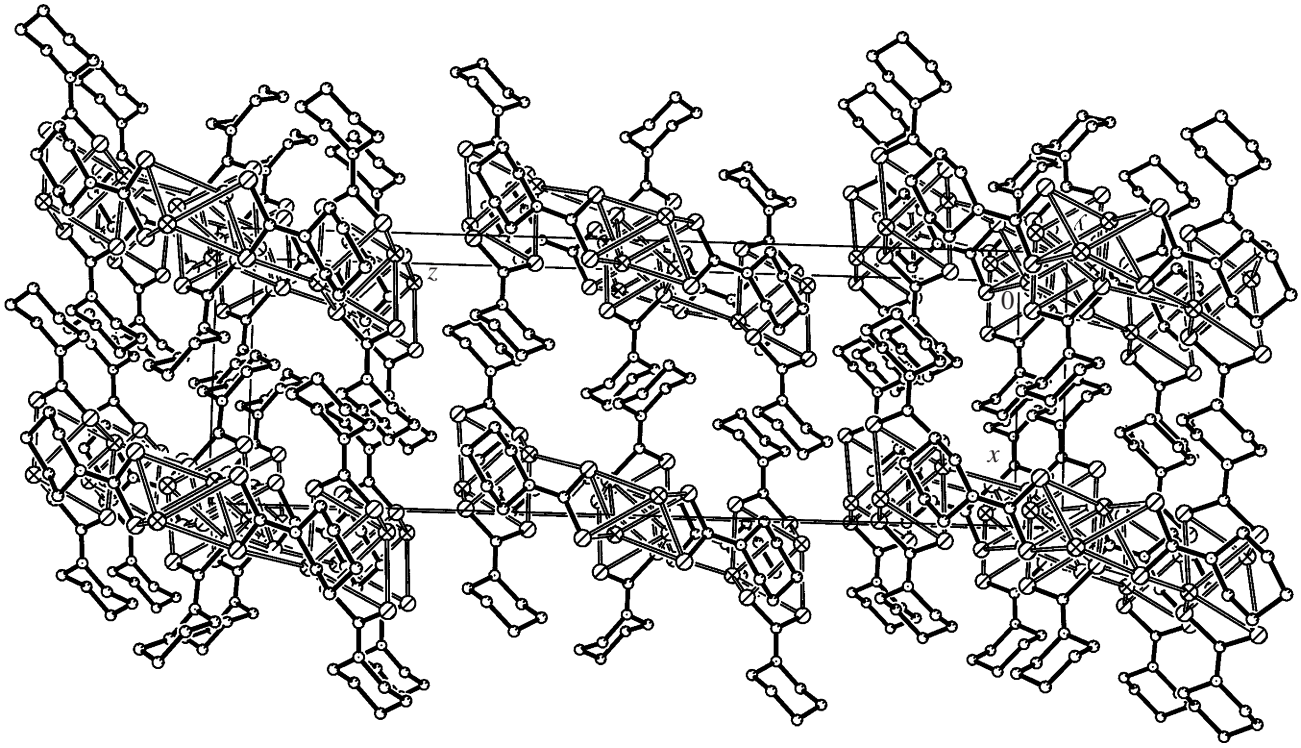

Fig. 2. Packing of the structural units in crystal **I** (projection to the *xz* plane).

δ = 201.5 ppm. The latter made it possible to reveal the internal structure of the discussed signal caused by a superposition of three (1 : 2 : 1) closely lying resonance lines (Fig. 1a, Table 3). The ^{15}N NMR spectrum (Fig. 1b) contains resonance signals with an intensity ratio of 2 : 1 : 1, which corresponds to the ^{13}C NMR spectrum. Moreover, the mathematical simulation of the ^{15}N NMR signal with δ = 140.0 ppm shows that this signal is the result of the summation of two (1 : 1) closely lying lines (Table 3). These data indicate that structure **I** contains four groups of the structurally nonequivalent PmDtc ligands, reflecting the complicated structural organization of complex **I** compared to other dithiocarbamate complexes. The X-ray diffraction method was used to determine this organization.

The structural unit of crystal **I** is a $[Tl_2\{S_2CN(CH_2)_5\}_2]$ binuclear molecule. The unit cell of the compound includes eight formula units (Fig. 2). Despite the pronounced structural similarity of the dimers discussed, they form three groups (4 : 2 : 2) of structurally nonequivalent molecules: A (with the Tl(1), Tl(2) atoms), B (Tl(3), Tl(3)^b), and C (Tl(4), Tl(4)^d) (Fig. 3, Table 2). The considered binuclear molecules are characterized by a distorted octahedral structure. Each atom Tl coordinates all the four sulfur atoms of two PmDtc ligands that form the equatorial plane of the Tl_2S_4 octahedron (the Tl atoms are localized in the axial positions). Thus, the dithiocarbamate groups perform the tetradentate bridging structural function. Each ligand in the dimer with each tallium atom forms one stronger Tl–S bond (2.915–3.086 Å) and one less strong Tl–S bond (3.026–3.278 Å). In the PmDtc ligands, the C_2NCS_2 groups are almost planar and the N–C(S)S bonds (1.305–1.364 Å) are appreciably stronger than N–CH_2 (1.447–1.483 Å). Both these facts reflect a substantial contribution of double bonding to the formally ordinary N–C(S)S bond (or, which is the same, sp^2- admixing to the sp^3-hybrid states of the nitrogen and carbon atoms). The $(CH_2)_5N$ six-membered cyclic fragments have a chair conformation.

Unlike the B and C centrosymmetric molecules, the A dimers are noncentrosymmetric and include two structurally nonequivalent PmDtc ligands. The Tl···Tl interatomic distances, which indirectly reflect the strength of the A/B/C binuclear molecules, are 3.6053/3.7270/3.7351 Å. For the Tl_2S_4 octahedra, these values determine the compression-type distortion along the Tl–Tl axis. The distances between the diagonally arranged sulfur atoms are 4.953 and 5.014/4.798 and 4.900/4.784 and 5.133 Å. The N–C(S)S bond lengths in the PmDtc ligands of the A/B/C binuclear molecules also differ substantially: 1.327 and 1.331/1.305/1.36 Å. The structural differences revealed between the A, B, and C binuclear molecules along with the considerable structural similarity make it possible to classify them as conformers (when the equilibrium state of the molecular system is achieved in two or several energetically similar and simultaneously existing spatial forms).

Tallium(I) in the dithiocarbamate complexes is characterized by high coordination numbers of five and six [1–7]. However, no coordination saturation in thal-

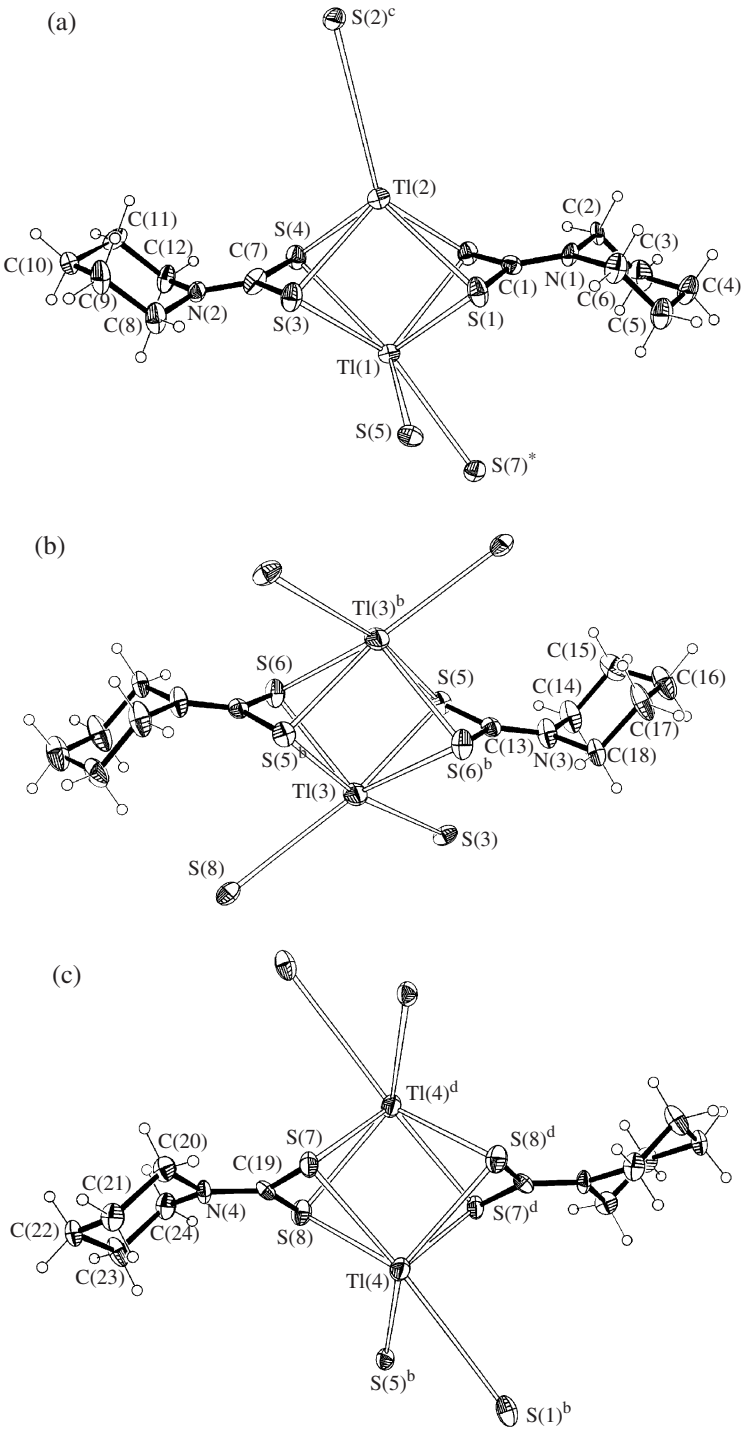

Fig. 3. Structures of binuclear molecules (a) A, (b) B, and (c) C.

lium is achieved in the $[Tl_2(S_2CNR_2)_2]$ binuclear molecules in spite of the coordination by the metal of all the four sulfur atoms. Therefore, the binuclear molecules associate to form more complicated (polynuclear) aggregates due to the additional Tl···S bonds. In our case, the further structurization of complex **I** produces zigzag polymeric chains along the *y* axis, whose formation involves the alternating centrosymmetric B and C dimers due to the Tl(4)–S(5)^b and Tl(3)–S(8) additional bonds (Fig. 4). The latter are less strong than the inner-dimer

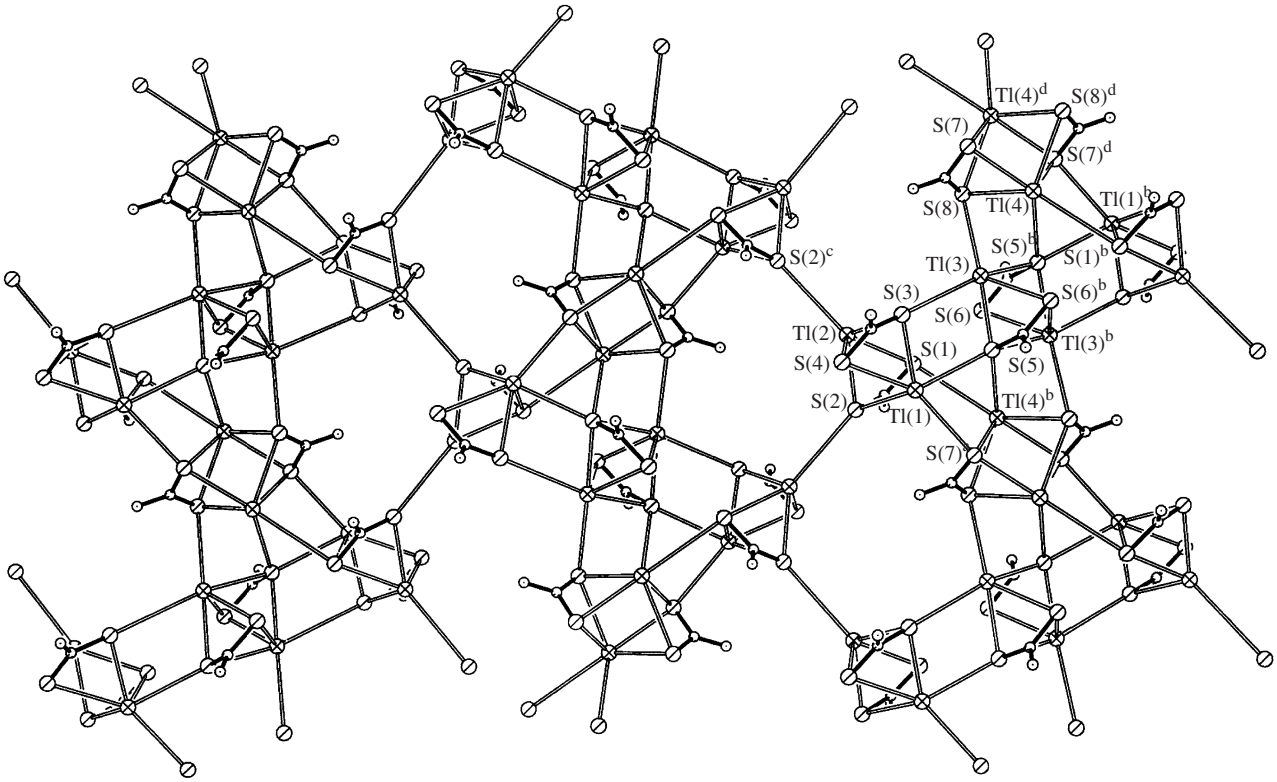

Fig. 4. Projection of structure **I** on the *yz* plane (the pentamethylene fragments are omitted for clarity).

bonds: 3.350 and 3.653 Å, respectively. The TlTlTl angles in the zigzag polymeric chain are 98.62° and 118.37°, and the Tl…Tl distances between the adjacent B and C molecules is 3.832 Å.

In turn, the polymeric chains are joined into dimeric layers due to the dimeric A molecules. The Tl(1) and Tl(2) atoms in the composition of the A dimer participate in a different manner in binding with the sulfur atoms of the binuclear B and C molecules (which compose the polymeric chains) and of the A molecule. Each Tl(1) atom forms two bonds with the sulfur atoms of the adjacent B and C dimers (Tl(1)–S(5) 3.447 and Tl(1)–S(7)^{a} (3.427 Å)), being fixed at the right and left from the polymeric chains with an increment of one unit. Each of the B and C dimers add one A dimer from both the right and left. In turn, the second Tl(2) atom of the dimeric A molecule forms only one additional bond with the sulfur atom of another A dimer localized from one side of the adjacent polymeric chain. These Tl(2)···S(2)^{c} (4.125 Å) are least strong.

It follows from the above presented data that the coordination number of the complexing agent in the complex is five (Tl(2) atom in the A molecule) and six (Tl(1) in A, Tl(3) in B, Tl(4) in C) (Fig. 3). The published data [1–7] make it possible to approximate the coordination polyhedra of the Tl(1), Tl(3), and Tl(4) atoms (coordination number six) by a distorted trigonal prism, and that of the Tl(2) atom (coordination number five) can be approximated by a distorted tetragonal pyramid.

The endotherm with an extreme at 180.9°C is observed in the DSC curve (Fig. 5b) before the beginning of thermal destruction. The independent measurement of the melting point shows that the enthotherm is caused by sample melting (176.9°C corresponds to the melting onset). The main weight loss of the sample occurs in the 306–320°C interval and starts from the relatively smooth region of the TG curve (Fig. 5a) with the transition at ~315°C to the steeply descending region: the DSC curve shows the maximum rate of the weight loss at 317.3°C. The discussed interval in the DSC curve (Fig. 5b) is presented by the endotherm with an extreme at 317.8°C caused by the thermal destruction of the sample and evaporation of the decomposition products. The pronounced asymmetry of the discussed effect reflects a complicated character of the reactions that occur during the thermolysis of the dithiocarbamate complexes [18, 19]. One more endotherm (with an extreme at 449°C) caused by the melting of the thallium(I) sulfide that formed is observed in the high-temperature region of the DSC curve: the melting onset corresponds to 445.5°C. (The decrease in mp compared to the reference values can be due to impurities.) The weight of the residue is 62.55% of the initial weight, which also agrees with the concepts on the formation of Tl_2S (the theoretical value is 60.44%) contaminated with the pyrolysis products.

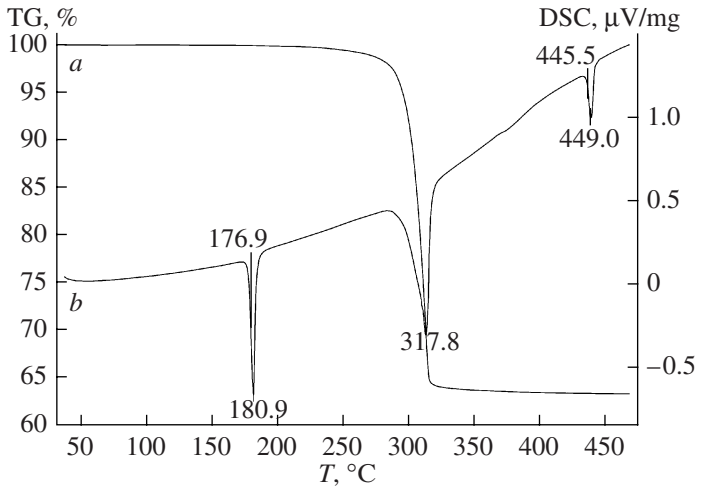

Fig. 5. The (*a*) TG and (*b*) DSC curves for complex **I**.

ACKNOWLEDGMENTS

This work was supported by the Russian Foundation for Basic Research (project no. 08-03-00068-a) and the Presidium of the Far East Division of the Russian Academy of Sciences (Program of Fundamental and Applied Research for Young Scientists, 2006–2008), grant no. 06-III-V-04-099.

REFERENCES

1. Ivanov, A.V., Bredyuk, O.A., Gerasimenko, A.V., et al., *Koord. Khim.*, 2006, vol. 32, no. 5, p. 354 [*Russ. J. Coord. Chem.* (Engl. Transl.), vol. 32, no. 5, p. 339].
2. Nilson, L. and Hesse, R., *Acta Chem. Scand.*, 1963, vol. 23, no. 6, p. 1951.
3. Jennische, P., Olin, A., Hesse R, *Acta Chem. Scand.*, 1972, vol. 26, no. 7, p. 2799.
4. Jennische, P. and Hesse, R., *Acta Chem. Scand.*, 1973, vol. 27, no. 9, p. 3531.
5. Anacker-Eickhoff, H., Jennische, P., and Hesse, R., *Acta Chem. Scand. A*, 1975, vol. 29, no. 1, p. 51.
6. Pritzkow, H. and Jennische, P., *Acta Chem. Scand. A*, 1975, vol. 29, no. 1, p. 60.
7. Elfwing, E., Anacker-Eickhoff, H., Jennische, P., and Hesse, R., *Acta Chem. Scand. A*, 1976, vol. 30, no. 5, p. 335.
8. Pines, A., Gibby, M.G., and Waugh, J.S., *J. Chem. Phys.*, 1972, vol. 56, no. 4, p. 1776.
9. Earl, W.L. and VanderHart, D.L., *J. Magn. Reson.,* 1982, vol. 48, no. 1, p. 35.
10. Morcombe, C.R. and Zilm, K.W., *J. Magn. Reson.,* 2003, vol. 162, no. 2, p. 479.
11. Ratcliffe, C.I., Ripmeester, J.A., and Tse, J.S., *Chem. Phys. Lett.*, 1983, vol. 99, no. 2, p. 177.
12. *SMART and SAINT-Plus. Version. 5.0. Data Collection and Processing Software for the SMART System*, Madison (WI, USA): Bruker AXS, 1998.
13. *SHELXTL/PC. Version. 5.10. An Integrated System for Solving, Refining and Displaying Crystal Structures from Diffraction Data*, Madison (WI, USA): Bruker AXS, 1998.
14. *Khimicheskaya entsiklopediya* (Chemical Encyclopaedia), Zefirov, N.S., Ed., Moscow: Bol'shaya Rossiiskaya Entsiklopedia, 1995, vol. 4, pp. 459, 491.
15. Ivanov, A.V., Gerasimenko, A.V., Konzelko, A.A., et al., *Inorg. Chim. Acta*, 2006, vol. 359, no. 12, p. 3855.
16. Ivanov, A.V. and Antzutkin, O.N., *Top. Curr. Chem.*, 2005, vol. 246, p. 271.
17. Ivanov, A.V., Kritikos, M., Antzutkin, O.N., and Forsling, W., *Inorg. Chim. Acta*, 2001, vol. 321, nos. 1–2, p. 63.
18. Skachkov, B.K., Oleinik, S.P., Matyna, L.I., et al., *Dokl. Akad. Nauk SSSR*, 1988, vol. 302, no. 5, p. 1149.
19. Oleinik, S.P., Matyna, L.I., Chistyakov, Yu.D., et al., *Dokl. Akad. Nauk SSSR*, 1989, vol. 307, no. 6, p. 1411.